RSC Advances

ROYAL SOCIETY OF CHEMISTRY

www.rsc.org/advances

Improvement of heat dissipation in agarose gel electrophoresis by metal oxide nanoparticles

Mohammad Zarei,[a] Elaheh K. Goharshadi, [a, b] Hossein Ahmadzadeh,[a,]* and Sara Samiee [a]

■ Author information

*Corresponding Author: h.ahmadzadeh@um.ac.ir

[a] Department of Chemistry, Ferdowsi University of Mashhad, Mashhad 91779, Iran

[b] Center of Nano Research, Ferdowsi University of Mashhad, Mashhad 91779, Iran

Abstract:

Joule heating is a primary limitation in the slab gel electrophoresis which is a gold standard method in biochemistry and biotechnology. In this paper, we introduced an innovative new class of heat transfer nanocomposite engineered by inclusion of metal oxide nanoparticles (NPs) in conventional separation medium (gel). The nanocomposite exhibits high thermal conductivity compared to gel itself. The results suggest a unique correlation between average particle size and thermal conductivity of metal oxide NPs with resolution improvement of the separation, i.e. reduction in Joule heating. Ceria, zirconia, tungsten oxide, and lanthania NPs were loaded into the agarose gel separately and used as a separation medium for gel electrophoresis. Among the NPs, ceria with the smallest size (5.2 nm) and highest thermal conductivity (17 W m^{-1} K^{-1}) presented a better performance in reduction of Joule heating. By loading 0.3 % (m/v) ceria, zirconia, and tungsten oxide NPs into the agarose gel at 25 $^{\circ}$C, the thermal conductivity of gel increased 79, 78, and 78 %, and resulted in 22, 18, and 14 % reduction in Joule heating (230 V), respectively. The overall separation efficiency and resolution increased for agarose/zirconia gel as compared with those of pure agarose gel. For example, the separation efficiency of 70 and 80 (bp) peaks increased 260 and 165 %, respectively. Also, the resolution increased from 1.65 for pure agarose gel to 6.32 for agarose/zirconia gel.

Keywords: Gel electrophoresis; Joule heating; Heat dissipation; Nanocomposite

1. Introduction

Agarose gel electrophoresis (AGE) is an important technique for separation of biological samples.[1] However, it suffers from some physical limitations leading to band broadening.[2] Joule heating is one of the most important factors in band broadening phenomenon. The heat generated is directly proportional to the separation voltage, electric current, and time. Heat dissipation in slab gel electrophoresis is an important goal to enhance the separation efficiency. Capillary gel electrophoresis (CGE) has been used to resolve this problem by efficient heat dissipation capability of the capillaries at the expense of higher cost of the instrument and the loss of high throughput capability of slab gel electrophoresis. Comparing to slab gel electrophoresis, CGE usually needs sophisticated and expensive instruments for the analysis of biomolecules.

The addition of nanoparticles (NPs) provides unique opportunities for substantially enhancing selectivity, efficiency, and stability of analytical techniques.[3] Application of NPs have been extensively studied in separation science.[4-9] Different types of NPs have been used successfully for the separation purposes such as carbon nanotubes,[10] fullerenes,[5] silica,[6] latex,[7] magnetic[11] and non-magnetic metal oxides,[12] silver[13] and gold NPs[14-17]. Also, polymer-based NPs have been used to coat silica capillaries in capillary electrophoresis.[18, 19] Surprisingly, very little research has been devoted to the application of NPs in slab gel electrophoresis.[8, 9]

The aims of the present study are to lower Joule heating by using nanocomposite gel with incorporation of the metal oxide NPs such as ceria (CeO_2), zirconia (ZrO_2), tungsten oxide (WO_3), and lanthania (La_2O_3) NPs in the agarose gel and calculate the separation efficiency. We focused on separation of two standard DNA samples (100 bp and 1000 bp) mixture of highly purified DNA fragments. We investigated the influence of NPs on porosity of agarose gel.

Thermal conductivity and Joule heating were calculated and temperature profile in gel was measured in order to understand the influence of NPs on thermal properties of separation matrix.

2. Materials and methods

2.1 Materials

All reagents were of analytical grade. Sodium borate, hydrochloric acid, ammonia, and ethidium bromide were purchased from Merck. Zirconyl nitrate and $LaCl_3.7H_2O$ were obtained from BDH Prolabo Chemicals. Tert-butyl alcohol and CTAB were purchased from Sigma-Aldrich. Sodium tungstate was purchased from Riedel. Agarose was purchased from KBC. GeneRuler 100 bp and 1 kb DNA standards were obtained from Fermentas and were subjected to electrophoresis without further treatment.

2.2 Agarose gel electrophoresis of nucleic acids

All separations were performed in slab gels (1 x 6 x 10 cm). DNA standard samples were analyzed on 1 % (m/v) agarose gel. The gels and the buffers contained 2.5 mM sodium borate buffer (pH=8.2). Nucleic acid samples were applied onto the gels in 10 pL 0.01 % (m/v) Bromophenol Blue for DNA. Gel images were analyzed using *ImageJ*[20] and *GelAnalyzer*[21] softwares.

2.3 Preparation of metal oxide NPs

Ceria NPs: 2.00 g cerium ammonium nitrate was dissolved in 20.0 ml deionized water. The NaOH solution (0.18 M) was added rapidly to the solution until white precipitate was formed. The reaction vessel was then placed into a microwave (Panasonic, model: NN-C2003S, Power: 1000 W) in the cycle mode of 10 s on and 5 s off (30 % power). The resulting precipitate was

centrifuged (10 min. with 13000 rpm) and washed with deionized water several times. Finally, the products were dried in a vacuum oven at 60 °C overnight.[22]

Zirconia NPs: The ZrO_2 NPs were prepared by hydrolysis of zirconyl nitrate in aqueous alcohol solution under microwave irradiation. 50.0 ml of $ZrO(NO_3)_2$ aqueous solution (0.2 M) was mixed with 200.0 ml of tert-butyl alcohol. This mixture was heated to the boiling point for 3 min. in microwave oven. Then, ammonia solution was added to the mixture to adjust the pH of solution to 9.0. Subsequently, the white precipitate was centrifuged, washed with deionized water, and dried in vacuum oven at 60 °C for 1 h. The obtained solid was calcined at 500 ^oC for 5 h.[23]

Tungsten oxide NPs: 30.0 ml hydrochloric acid aqueous solution (4 M) was added to 20 ml aqueous solution of sodium tungstate, $Na_2WO_4.2H_2O$ (0.05 M) and stirred for 1 h at 25 °C. The solution was introduced into a Teflon tube and autoclaved for 24 h at 80 °C. The yellow precipitate was separated by centrifuging, several times washing with distilled water, and air-drying in a furnace (3 h, 250 °C).

Lanthania NPs: 0.27 g of CTAB was added to 30.0 mL distilled water under magnetic stirring (25 °C). Then, 1.58 mmol $LaCl_3.7H_2O$ was added to the solution to form a homogeneous transparent solution. In order to adjust the pH of the solution to 8.5, ammonia (25 %) was added dropwise to the above solution and stirred for 2 h and then transferred into a Teflon lined stainless steel and autoclaved for 24 h at 80 ºC. The white solid product was centrifuged, washed with distilled water, and dried in vacuum oven for 4 h at 80 ºC. Finally, the resultant powder was calcined (4 h, 800 ºC).[24]

2.4 Synthesis of nanocomposite hydrogel

In a typical synthesis, 0.20 g agarose was dissolved in 20.0 mL sodium borate buffer (2.5 mM) and heated to 80 °C for 10 min. The proper amount (0.1 - 0.3 % (m/v)) of each NPs was rapidly added to the agarose solution. Then, the agarose/NPs solution was cooled down to room temperature. The temperature probe (Misonix S-400) was used to measure the temperature in different positions of the gel (from cathode to anode).

2.5 Characterization methods

The X-ray diffraction measurements were performed by Bruker/D8 Advanced diffractometer in the 2θ range from 20^o to 80^o, by 0.04 degree steps, using graphite monochromatic Cu Kα radiation (λ= 1.541 Å). The transmission electron microscopy (TEM) analysis of the samples was carried out on a LEO 912 AB transmission electron microscope with the electron beam accelerating voltage of 120 kV.

3. Results and discussion

3.1 Characterization

Fig. 1 shows the XRD patterns of ceria, zirconia, tungsten oxide, and lanthania NPs. In general, no additional peaks in the XRD patterns of the samples were observed which can be related to the high purity the NPs. Also, the peaks of the NPs are sharp and strong which indicate the high crystallinity of the samples. The diffraction peaks of ceria NPs (Fig. 1a) could be indexed to the face-centred cubic phase with the lattice parameter of $a = b = c = 0.5410$ nm.

The average crystallite size of the prepared NPs was estimated using the Scherrer formula: [25]

$$D_{hkl} = \frac{k \times \lambda}{\beta_{hkl} \times \cos\theta_{hkl}} \quad (1)$$

where k is a constant (0.9), D_{hkl} is the particle size perpendicular to the normal line of (hkl) plane, θ_{hkl} is the Bragg angle of (hkl) peak, β_{hkl} is the full width at half maximum of the (hkl) diffraction peak, and λ is the wavelength of X-ray. The average crystallite size of ceria NPs was calculated as 5 nm. The diffraction peaks of the zirconia NPs were indexed to (011), (111), (002), (220), (211), (112), (220), (222), (013), and (131) reflections which correspond to purely monoclinic phase. The average crystallite size of zirconia NPs was about 21 nm. The diffraction pattern of tungsten oxide NPs (Fig. 1c) with average crystallite size of 25 nm was corresponded to the monoclinic phase. The diffraction peaks of lanthania NPs (Fig. 1d) with average crystallite size of 28.8 nm were indexed to (100), (002), (101), (102), (110), (103), (112), (004), (202), and (104) reflections assigning to the hexagonal phase with the lattice parameters of a=b=0.3973 nm and c =0.6129 nm.

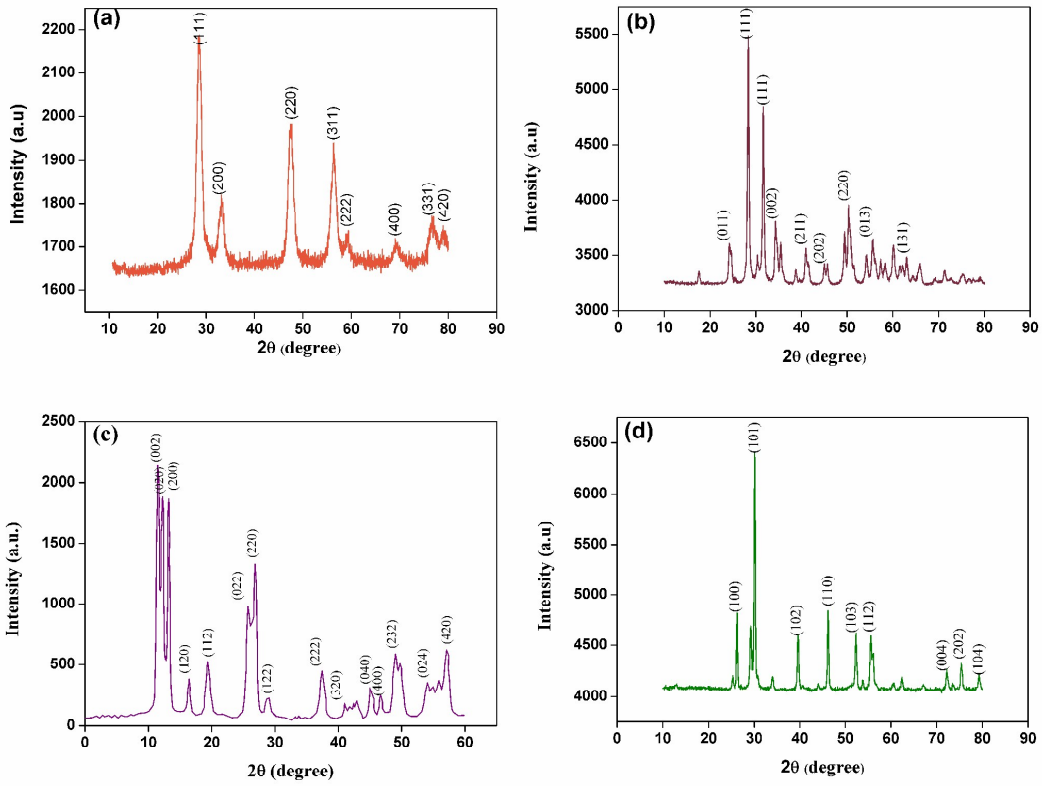

Fig. 1 The XRD patterns of (a) ceria, (b) zirconia, (c) tungsten oxide, and (d) lanthania NPs.

Fig. 2 shows TEM images with the embedded particle size distribution of ceria, zirconia, tungsten oxide, and lanthania NPs. According to these images, the NPs display the uniform morphology with the average size of 5.2, 26, 31.5, and 51.2 nm for ceria, zirconia, tungsten oxide, and lanthania NPs, respectively.

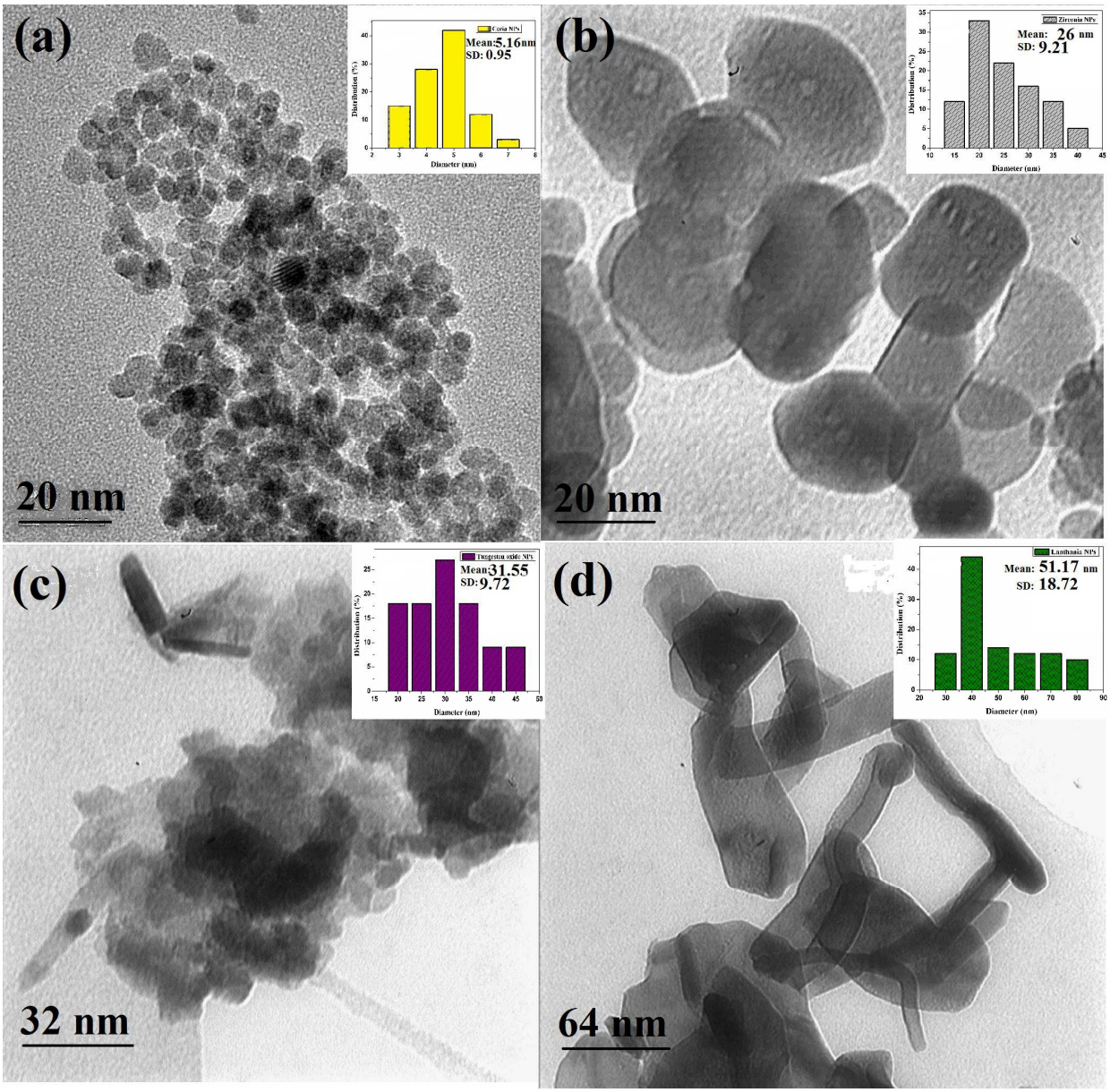

Fig. 2 The TEM images and particle size distribution of prepared (a) ceria, (b) zirconia, (c) tungsten oxide, and (d) lanthania NPs.

3.2 Joule heating

In order to study the Joule heating effect, Ohm's plot was constructed by applying different voltages across the separation medium and monitoring the generated currents. Fig. 3 shows *I-V* measurement (Ohm's plot) for the agarose gel and the agarose/NPs modified gels. A threshold voltage (U_t) above which the current begins to abruptly increase is the maximum separation voltage that should be applied in order to having the shortest separation time. The values of U_t in the pure agarose and the agarose/ceria, agarose/zirconia, agarose/tungsten oxide, and agarose/lanthania gels were estimated to be 170, 200, 190, 180, and 175 V, respectively. At high voltages, produced heat in the NPs embedded gels is less than that of the pure agarose gel (Fig. 3 a-d). The heat generated, is directly proportional to the separation voltage, *U*; electric current, *I*; and time, *t*:

$$q = U\ I\ t \tag{2}$$

Fig. 3 (e-h) shows the calculated Joule heating for the pure agarose gel and the NPs embedded gels at different applied voltages. As this figure shows by addition of the NPs to the agarose gels, the amount of Joule heating decreased. For example, at 150 V, the value of generated heat were 16.31, 15.39, 16.17, 16.20 kJ for agarose, ceria/agarose, zirconia/agarose, tungsten oxide/agarose, and lanthania/agarose gels, respectively. The significant decrease in Joule heating is seen at higher applied voltages. For example, at 220 V the value of produced heat were 18.46, 16.42, 16.75, 16.93, and 16.85 kJ in agarose, ceria/agarose, zirconia/agarose, tungsten oxide/agarose, and lanthania/agarose gels, respectively. In ceria/agarose gel, the produced heat reduces 6 and 12 % at 150 V and 200 V, respectively.

By increasing the percentage of NPs loading, the magnitude of Joule heating decreases further. By loading 0.3 % m/v of the NPs, at applied voltages, the value of Joule heating

decreased 12, 10, 9, and 8 % for agarose/ceria, agarose/zirconia, agarose/tungsten oxide, and agarose/lanthania gels, respectively compared to that of the pure agarose gels. The order of decrease in Joule heating has a good correlation with the average particle size and thermal conductivity of the NPs. As Table 1 shows, there is a correlation between average particle size and thermal conductivity of metal oxide NPs with reduction in Joule heating. The ceria NPs with the smallest size and highest thermal conductivity among the NPs reduced the Joule heating by 12 % when 0.3 % m/v included into the gel. Even at higher voltage 230 V, by loading 0.3 % m/v ceria NPs into the agarose gel at 25 $^{\circ}$C, the thermal conductivity increased 79 %, which resulted in 22 % reduction in Joule heating and increase of separation efficiency. Generally, Joule heating increases with applied voltage but in the NPs modified gels, NPs acts as heat sinks and reduce the generated heat. The thermal conductivity of the metal oxide NPs increases significantly with temperature as well as the volume fraction of NPs.[26] This leads to reduction of Joule heating by agarose/metal oxide NPs gel at high voltages.

The temperature difference between the center line and the inside line of separation medium can be calculated by *Knox* equation:[27]

$$\Delta T = \frac{Q r^2}{4 \kappa} \tag{3}$$

where r is radius of separation medium, κ is thermal conductivity, and Q is the heat produced per unit volume and time:

$$Q = \frac{U I}{w h l} \tag{4}$$

where w, h, and l are dimensions of gel. As Eq. 3 shows there is an inverse relationship between temperature difference and thermal conductivity of medium. Hence, thermal conductivity plays a vital role for improvement of separation. The thermal conductivity of the NPs is higher than that

of pure agarose gel (0.56 W m^{-1} K^{-1})[28]. Of course, choosing appropriate NPs is very important. For example, the carbon nanotubes (CNTs) were included into separation gels [29, 30] to improve the resolutions of serum DNAs.

The main criterion is choosing NPs with high thermal conductivities and low electrical conductivities. The reason is simple; we do not wish the NPs move and/or cause non-uniformities in electric field, i.e. NPs with low electrical conductivities. At the same time, we wish the NPs act as heat sinks to effectively dissipate heat and lower Joule heating, i.e. NPs with high thermal conductivities. Based on this criterion, ceria, zirconia, tungsten oxide, and lanthania NPs were chosen (Table 1).

Table 1 Correlation between average particle size and thermal conductivity of the NPs with the decrease in the magnitude of Joule heating

NPs	Average particle size (nm)[a]	Thermal conductivity of the bulk (W m^{-1} K^{-1})	Electrical conductivity of the bulk (S m^{-1})	Joule heating reduction (%)
CeO_2	5.2	17 [31]	0.044 [32]	12
ZrO_2	26.0	4.2 [33]	0.86 [34]	10
WO_3	31.5	1.6 [35]	NR[b]	9
La_2O_3	51.2	NR	10^{-5} [36]	8

[a] Calculated using TEM image.
[b] Not reported

There is an important disadvantage of using CNT in separation medium. CNT has high thermal conductivity (3500 W m^{-1} K^{-1})[37] and high electrical conductivity (10^6-10^7 S m^{-1})[38]. The CNTs move when the separation voltage is applied. That causes the depletion of CNTs on one side of the gel and accumulation on the other side. If voltage is applied for a long time, the CNTs keep moving and might egress from other side of the gel. The Joule heating would be lower on the

side where the CNTs have migrated to and higher on the depleted side. In this work, we chose the metal oxide NPs since they have high thermal conductivity but low electrical conductivity. Hence, metal oxide NPs increase the thermal conductivity of separation medium without generation of concentration gradient across the gel.

The temperature difference between the center and the edges of gels measured by temperature probe and calculated by *Knox* equation (Eq. 3) is shown in Fig. 4. The temperature gradient in the agarose/metal oxide NPs is smaller than that of pure agarose due to higher thermal conductivity of the NPs (Fig. 4). At 200 V, the temperature gradient across the agarose/ceria, agarose/zirconia, agarose/tungsten oxide, and agarose/lanthania gels was 0.20, 0.35, 0.60, and 1.00 °C, respectively while 2.5 °C in pure agarose gel when the loading amount of NPs was 0.1 % m/v. For loading amount of 0.3 % m/v, temperature gradient across the agarose/ceria, agarose/zirconia, agarose/tungsten oxide, and agarose/lanthania gels was 0.17, 0.28, 0.41, and 0.77 °C, respectively. By increasing the percentage NPs loading from 0.1 to 0.3 % m/v, the temperature gradient in gel reduced further. This is related to the higher values of thermal conductivity of the gel/NPs than that of pure agarose gel.

There are no theoretical formulas to predict the thermal conductivity of the suspensions of NPs, so-called nanofluid, satisfactorily.[39] The Maxwell model[40], a traditional model for thermal conductivity, was proposed for solid–liquid mixtures:

$$\lambda_c = \frac{\lambda_f + 2\lambda_m + 2\phi(\lambda_f - \lambda_m)}{\lambda_f + 2\lambda_m - \phi(\lambda_f - \lambda_m)} \quad (5)$$

where λ_f and λ_m are the thermal conductivity of the nanocomposite (agarose/NPs gel), filler material (NPs), and polymer matrix (agarose), respectively. The Maxwell model underestimates

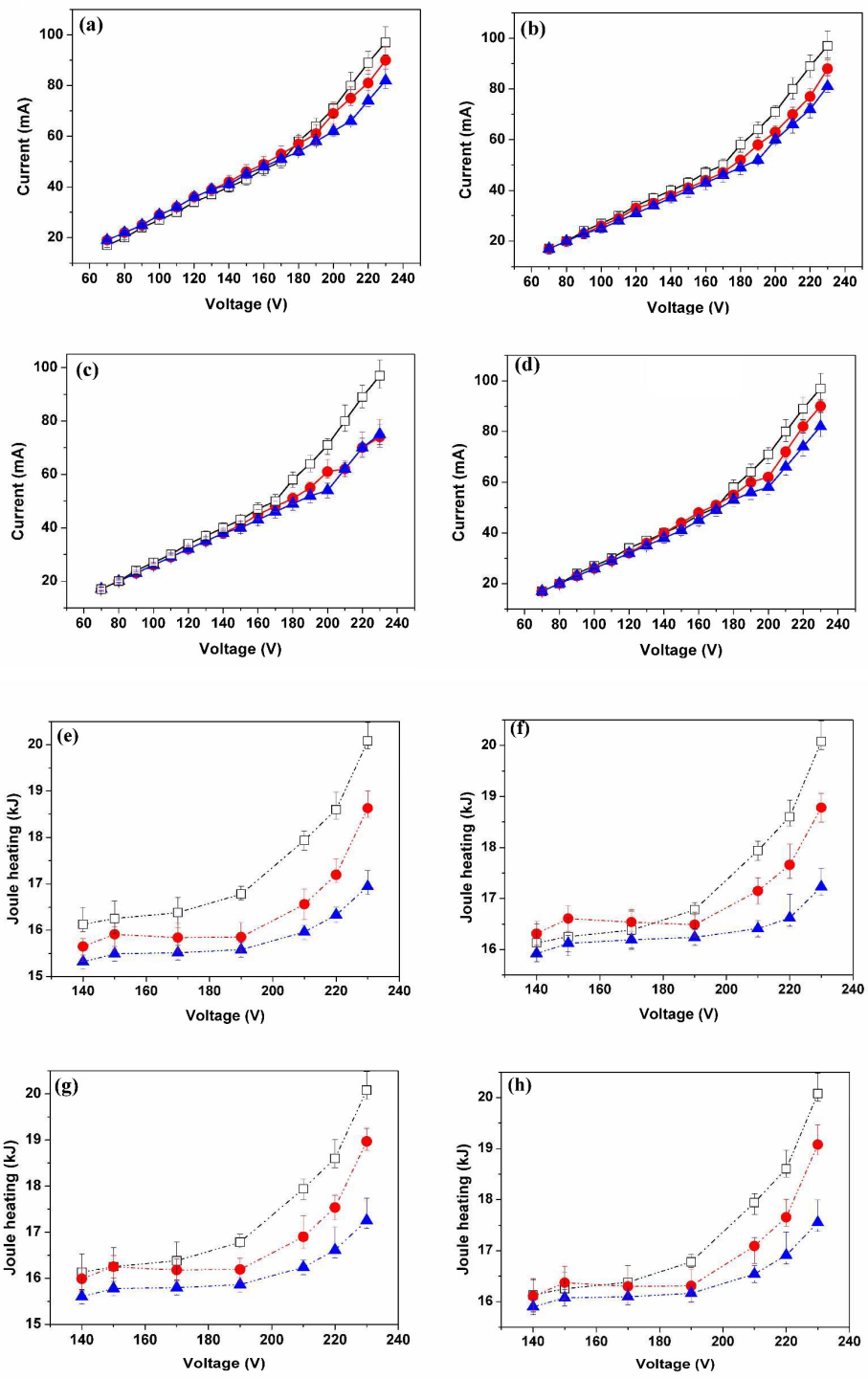

Fig. 3 Current *vs* voltage curve for (a) agarose/ceria (b) agarose/ zirconia (c) agarose/ tungsten oxide (d) agarose/lanthania and the magnitudes of Joule heating versus applied voltage for (e) agarose/ceria (f) agarose/zirconia lanthania (g) agarose/ tungsten oxide (h) agarose/ lanthania (□ pure agarose, ● = 0.1, ▲ = 0.3 % m/v).

the thermal conductivity of the suspensions of NPs. This is because the model does not include the effects of particle size, particle size distribution, and temperature.[41]

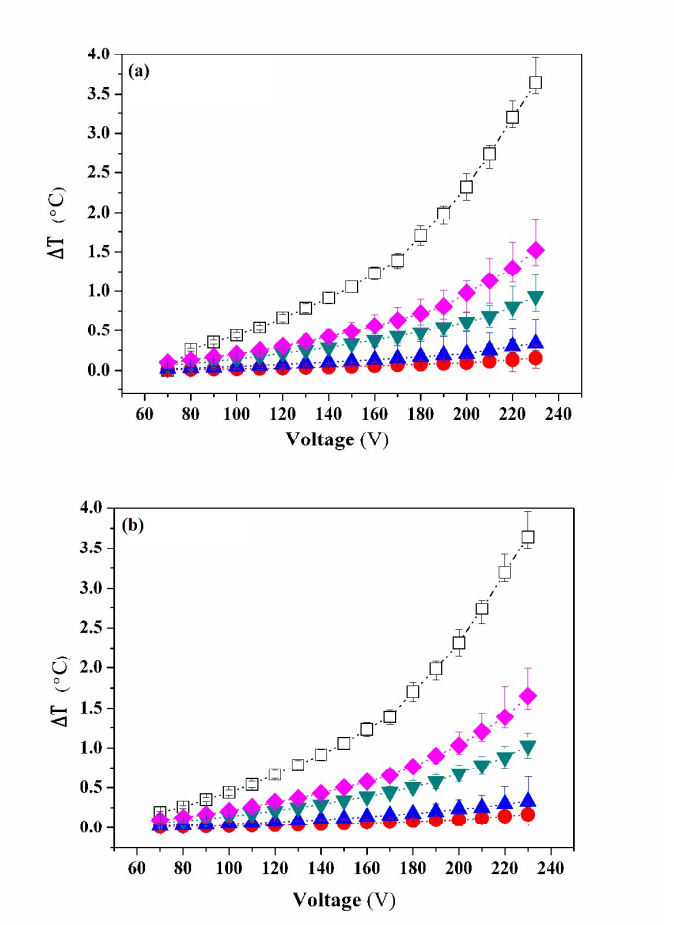

Fig. 4 Temperature difference between the center and the edges of gels at (a) 0.1 % (m/v) (b) 0.3 % (m/v) (□ agarose, ● agarose/ceria, ▲ agarose/zirconia, ▼ agarose/ tungsten oxide, and ◆ agarose/lanthania gels).

The thermal conductivity of agarose/ceria, agarose/ zirconia, and agarose/tungsten oxide was calculated according to the Maxwell model as 1.0010, 1.0003, and 1.0061 for 0.3 % (m/v) of the NPs, respectively. This is equivalent to 79 % for agarose/ceria, 78 % for agarose/zirconia, and 78 % for agarose/tungsten oxide gels enhancement in thermal conductivity compared with that of the agarose gel. Hence, the NPs act as heat sinks to lower the produced heat. After careful

analysis with respect to the Joule heating and thermal conductivity measurements, agarose/ceria and agarose/zirconia nanocomposite gels were chosen as separation medium for separation of DNA samples.

3.3 Separation of standard DNA samples by the NPs modified gels

The separation panels and electropherograms of standard DNA samples (a mixture of 10, highly purified DNA fragments (100 bp: 10 bp-100 bp and 1 kb: 100 bp-1000 bp) on agarose gel and the agarose gel/NPs are shown in Fig. 5. The separations were performed at different voltages (170, 210, and 200 V for agarose, agarose/ceria, and agarose/zirconia, respectively) chosen based on the threshold voltage for the initiation of Joule heating for agarose and agarose/NPs. Also, we compared the performance of the agarose/NPs with that of pure gel for separation in high voltages. For separation of 1 kb DNA sample **(**Fig. 5 a-c**)**, the number of separated DNA fragments in the range of 700-1000 bp increased for agarose/ceria and agarose/zirconia compared to those of the pure agarose gel. Also, the separation time decreases in the agarose gel/NPs compared to that of the pure agarose gel because of higher applied voltages. In separation of 100 bp DNA sample, the number of separated DNA fragments increased in agarose /ceria compared to that of the pure agarose gel (Fig. 5 d-f).

The efficiency of the electrophoresis can be evaluated by the number of theoretical plates, N:[2]

$$N = 5.54\left(\frac{t}{w_{1/2}}\right)^2 \quad (6)$$

where t and $w_{1/2}$ stand for migration time of the DNA fragments and the temporal peak widths at half of the peak heights. The number of theoretical plates for the peaks 10-100 and 100-1000 for agarose, agarose/ceria, and agarose/zirconia gels are given in Table 2. The values of N increased

in agarose/zirconia gel compared to those of agarose gel. The number of theoretical plates, N is related to the applied voltage, U by the following equation:[42]

$$N = \frac{z F U}{2\theta R T} \quad (7)$$

where z *is* effective charge, F, the Faraday constant or charge per mole of protons, T is temperature, R *is* gas constant, and θ is dispersion coefficient. In electrophoresis, efficiency (N) increases by increasing voltage as far as Joule heating allows. By incorporation of metal oxide NPs into the agarose gel, the Joule heating threshold voltage expands. This maximizes the separation efficiency and lowers the separation time.

The resolution between two peaks in electropherogram can be calculated as:[2]

$$R_s = \frac{2(t_2 - t_1)}{w_1 + w_2} \quad (8)$$

where t_1 and t_2 are the migration times for components 1 and 2, respectively. w_1 and w_2 stand for the temporal peak widths of components 1 and 2, respectively. The appropriate resolution between components requires a combination of good selectivity and good separation efficiency ($R_s \sim N^{1/2} \sim U^{1/2}$).[43, 44] Resolution between peaks was also measured. In general, the resolutions increased in agarose/zirconia gel compared to those of the agarose gel. For example, the resolution between peaks 70 and 80 (bp) was increased from 1.65 for pure agarose gel to 6.32 in agarose/zirconia gel.

Close examination of the bands shows broad peaks for agarose gel whereas this broad peaks split into partially resolved peaks in agarose/zirconia gel. This shows the enhancement in resolution where the metal oxide NPs are embedded in agarose gel. For separation of 1 kb and 100 bp DNA fragments using agarose/zirconia gel electrophoresis, resolution for all adjacent

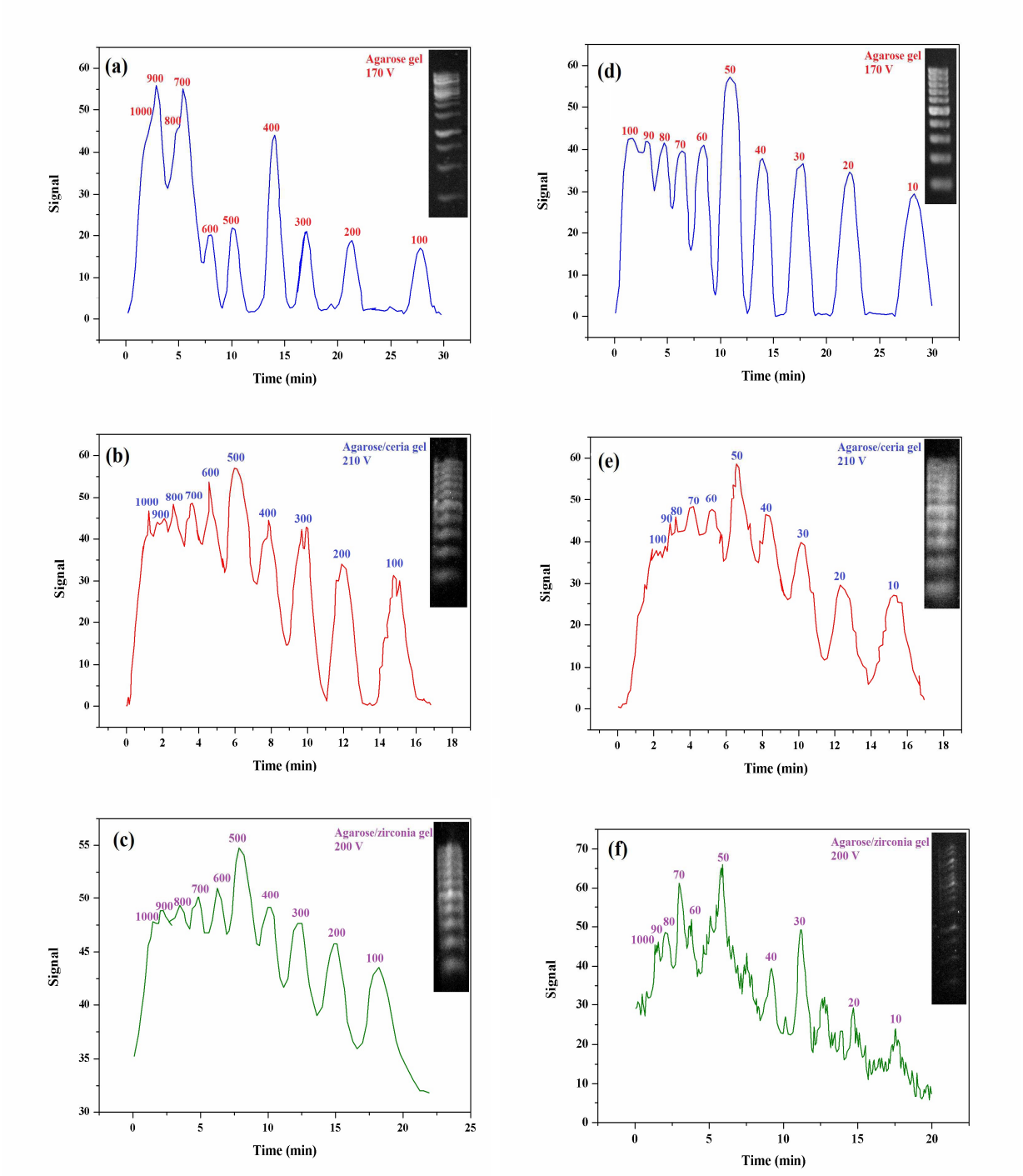

Fig. 5 The electropherograms of standard DNA sample (1 kb) on the (a) pure agarose (b) agarose/ceria (c) agarose/ zirconia, 0.3 % m/v (numbers: number of base-pairs). The electropherograms of DNA sample (100 bp) on the (d) pure agarose (e) agarose/ceria (f) agarose/ zirconia, 0.3 % m/v (numbers: number of base-pairs).

pairs was calculated. The results are tabulated in Table 3 and shown in Fig. 5. The separation parameters in agarose gel/zirconia and the number of separated DNA fragments significantly increased as compared to the pure gel. The number of separated DNA fragments for separation at 210 V, increased in agarose gel/ceria (0.3 % m/v) compared to the pure gel. There is a significant decrease in analysis time at higher voltages with the NPs modified gel. For example, the separation time of DNA 100 (bp) by agarose, agarose/ceria, and agarose/zirconia is 30, 17, and 22 min. and for DNA 1 (kb) is 30, 17, and 20 min., respectively. Also, the sharpness of peaks increased in agarose gel/ceria. The number of peaks for separation of long-stranded DNA fragments (100 bp: 70-100 bp, 1000 bp: 700-1000 bp) increased in both agarose/ceria and agarose/zirconia gels compared to that of agarose gel.

The effective separation of long-stranded DNA fragments is important in comprehensive genomic analysis of DNA samples and is operated usually by pulsed field gel electrophoresis.[45] Unfortunately, pulsed field gel electrophoresis is slow and separation times are in the range of several hours to several days. Although capillary electrophoresis (CE) with entangled polymer[46] solutions was used for the separation of DNA molecules of different sizes [47-49] but CE is not efficient for separations of long-stranded DNA due to the needs to sophisticated and expensive instruments. The ultradilute polymer solutions,[50, 51] pulsed-field CE,[52-54] entropy trap arrays,[55, 56] asymmetric obstacle arrays[57] and a DNA prism,[58] have been developed to overcome the problem of time delays in CE.

Table 2 Calculated theoretical plate number of standard DNAs.

Peak (bp)	*N*		
	Agarose gel	Ceria NPs (0.3 % m/v)	Zirconia NPs (0.3% m/v)
100	354.56	101.75	176.32
200	610.78	132.65	345.36
300	400.26	124.32	246.32
400	173.73	1418.24	110.65
500	138.50	110.78	121.32
600	311.60	632.12	187.32
700	16.78	1418.81	26.32
800	……	1246.50	45.29
900	2.82	554.00	72.32
1000	……	640.12	69.31
10	694.93	265.12	2650.97
20	608.00	285.63	4989.56
30	384.56	177.32	3462.50
40	126.70	101.32	2681.36
50	122.65	234.06	3512.36
60	77.90	138.62	2216.21
70	54.10	354.56	482.59
80	43.43	635.32	384.70
90	73.12	452.31	670.34
100	46.32	532.15	571.25

Table 3 Measured resolution of adjacent bands for standard DNAs.

Peak (bp)	R_s		
	Agarose gel	Ceria NPs (0.3 % m/v)	Zirconia NPs (0.3% m/v)
100-200	2.54	1.57	1.09
200-300	2.00	1.11	1.62
300-400	2.12	1.20	1.33
400-500	1.33	1.60	1.25
500-600	1.66	0.66	0.57
600-700	0.5	1.32	0.65
700-800	……	4.12	0.55
800-900	……	2.32	1.06
900-1000	……	4.65	1.12
10-20	2.58	1.55	3.33
20-30	2.10	1.50	3.56
30-40	2.15	1.62	3.00
40-50	2.32	1.55	4.12
50-60	1.71	1.12	4.28
60-70	1.62	1.09	5.12
70-80	1.65	2.59	6.32
80-90	1.81	2.01	2.31
90-100	0.65	2.25	1.23

Huang et al.[59] separated the long double-stranded DNA (dsDNA) molecules by nanoparticle-filled capillary electrophoresis. They used gold nanoparticles (GNPs) modified with poly (ethylene oxide) (PEO) to form gold nanoparticle/polymer composites (GNPPs). The GNPPs are

heavy and electrically neutral: thus, slow down the DNA molecules migration in the electrophoresis. Polymer solutions such as PEO and the GNPPs provide greater efficiency and shorter migration times for separation of long dsDNA. Polymer chains could attach to the surfaces of the NPs through their hydrophobic parts, which leaves their hydrophilic groups available to interact with the polar dispersion media.

The NPs can be wrapped with long single- and double-stranded DNA (ssDNA and dsDNA). The ssDNA and dsDNA have different affinities to NPs.[60] The essential difference in adsorption behavior between ssDNA and dsDNA may be attributed to their different electrostatic properties. Also, the ssDNA has a flexible structure and uncoils in solution under the influence of applied voltage. In contrast, dsDNA has stable and rigid structure.[61] For example, long ssDNA can wrap around CNTs.[62, 63] Hence, it is plausible to say that the large ssDNA fragment may adsorb onto the NPs and trapped by NPs.

The polymer chains are adsorbed on the surface of metal oxide NPs to form the NPs/ polymer composite. The composite is heavy and electrically neutral, hence slows the migration of the DNA molecules. Long DNA fragments have a greater probability to interact with more than one NPs depending on the DNA size and conformation. The drag force is stronger for long DNA fragments as compared to short ones. As a result, the mobility of long DNA is smaller than that of a short one. Fig. 5 shows that for agarose/ceria gel, the resolution and efficiency of DNAs with higher molecular weights (700-1000 bp) are greater as compared with lower molecular weights (100-600 bp) which could be explained by interaction of long stranded DNAs with NPs surface.

Incorporation of NPs in separation medium could change the physicochemical behavior and thermal conductivity of separation medium.[8]

3.4 Influence of the NPs concentration

In order to understand the relationship between the NPs concentration and the degree of improvement in separation parameters, three different concentrations of NPs (0.1, 0.3, and 0.5 % m/v) were incorporated into agarose gel. The optimum separation efficiency was obtained for 0.3 % m/v of the NPs. However, when the concentration of the NPs is higher than 0.3 % m/v, no significant improvement in separation parameters was achieved. The excess NPs concentration will make an interference with UV light produced by gel documentation system which increases the background of images and lowers the S/N ratio of separation profiles.

3.5 Influence of NPs on gel porosity

In order to understand the influence of NPs incorporation on porosity of the agarose gel, the porosity was calculated by measuring the density of dry and wetted gels. The overall gel porosity was calculated with the following formula: [64]

$$\%Porosity = \frac{dry\ density - wetted\ density}{density\ of\ water} \times 100 \quad (9)$$

The wetted density is the ratio of the weight and volume of a gel which was saturated with a wetting liquid for 24 h at room temperature. Table 4 shows that porosity in water increases with the amount of the NPs filler. For example, in a gel containing 0.1 and 0.3 % m/v of ceria NPs, the porosity increased by 2 and 3 % with increasing filler content. The porosity of gel was increased by increasing the amount of NPs. In general, the sharpness and resolution of all defined bands increased in the NPs modified gel because the NPs alter both the chemical composition and thermal conductivity of the polymer matrix.

Table 4 Porosity variations in NPs embedded gels for different NPs concentration.

Matrix	Porosity enhancement	
	0.1 % m/v	0.3 % m/v
Agarose/ceria	2	3
Agarose/tungsten oxide	1	2
Agarose/zirconia	2	4

By introducing the NPs into the matrix, the pore size distribution of matrix changes with respect to the pure gel. The inclusion of the NPs has been shown to cause nucleation which reduces the pore size of polymer matrix[65]. Also, as the size of NPs decreases, the pore density increases compared to that of the gel.

4. Conclusions

Metal oxide NPs were embedded into the agarose gel to increase the separation efficiency by reducing Joule heating and lowering band broadening. The influence of NPs on the Joule heating was successfully evaluated. The reduction of Joule heating was observed by dispersing the NPs in the agarose gel. The results showed a unique correlation between the average particle size and thermal conductivity of the metal oxide NPs with reduction in the amount of generated heat. Among the metal oxide NPs, ceria with the smallest size (5.2 nm) and highest thermal conductivity (17 W m^{-1} K^{-1}) presented a better performance in lowering the Joule heating.

The optimum separation efficiency was obtained for 0.3 % m/v of the NPs. For example, by loading 0.3 % m/v ceria NPs in agarose gel at 25 ^{o}C, the thermal conductivity increased up to 79 % which resulted in 22 % reduction in Joule heating and an increase in separation efficiency.

Finally, this paper presents a potential to improve the separation efficiency and resolution of other biomolecules using slab gel electrophoresis.

Acknowledgements

The authors acknowledge ATF committee and Ferdowsi University of Mashhad for supporting this project (3/23032). The authors also thank Dr. Razieh Jalal and Dr. Ahmad Reza Bahrami for generous donation of DNA standards.

Notes and references

1. B. D. Hames, *Gel Electrophoresis of Proteins: A Practical Approach: A Practical Approach*, Oxford University Press, 1998.
2. R. Kuhn and S. Hoffstetter-Kuhn, *Capillary Electrophoresis: Principles and Practice*, Springer-verlag, Berlin, 1993.
3. C. R. Martin and D. T. Mitchell, *Anal. Chem.*, 1998, **70**, 322A-327A.
4. L. Yang, E. Guihen, J. D. Holmes, M. Loughran, G. P. O'Sulliva and J. D. Glennon, *Anal. Chem.*, 2005, **77**, 1840-1846.
5. M. R. Ivanov, J. H. Amanda, *Analyst,* 2011, **136,** 54-63.
6. L. Tang, X. Wang, B. Guo, M. Ma, B. Chen, S. Zhan, & S. Yao, *RSC. Adv.*, 2013, **3,** 15875-15886.
7. D. Xiao, C. Zhang, D. Yuan, J. He, J. Wu, & H. He, *RSC. Adv.*, 2014, **4,** 64843-64854.
8. M. Zarei, H. Ahmadzadeh and E. K. Goharshadi, *Analyst*, 2015, **140**, 4434-4444.
9. M. Zarei, H. Ahmadzadeh, E. K. Goharshadi and A. Farzaneh, *Anal. Chim. Acta.*, 2015, **887**, 245-252.
10. H. Luo, Z. Shi, N. Li, Z. Gu and Q. Zhuang, *Anal. Chem.*, 2001, **73**, 915-920.
11. A. Manbohi, S. H. Ahmadi, and V. Jabbari, *RSC. Adv.,* 2015, **5,** 57930-57936.
12. A. Kolmakov and M. Moskovits, *Annu. Rev. Mater. Res.*, 2004, **34**, 151-180.
13. A. D. McFarland and R. P. Van Duyne, *Nano. Lett.*, 2003, **3**, 1057-1062.
14. E. Guihen and J. D. Glennon, *Anal. Lett.*, 2003, **36**, 3309-3336.
15. T. B. L. Kist and M. Mandaji, *Electrophoresis*, 2004, **25**, 3492-3497.
16. V. Sharma, K. Park and M. Srinivasarao, *Mater. Sci. Eng.*, 2009, **65**, 1-38.
17. C.-S. Wu, F.-K. Liu and F.-H. Ko, *Anal. Bioanal. Chem.*, 2011, **399**, 103-118.
18. G. Kleindienst, C. G. Huber, D. T. Gjerde, L. Yengoyan and G. K. Bonn, *Electrophoresis*, 1998, **19**, 262-269.
19. C. G. Huber, A. Premstaller and G. Kleindienst, *J. Chromatogr. A.*, 1999, **849**, 175-189.
20. M. D. Abràmoff, P. J. Magalhães and S. J. Ram, *Biophoton. Int.*, 2004, **11**, 36-43.
21. Lazar, I. Lazar, Gel Analyzer 2010a: Freeware 1D Gel Electrophoresis Image Analysis Software, 2012.
22. E. K. Goharshadi, S. Samiee and P. Nancarrow, *J. Colloid. Interf. Sci.*, 2011, **356**, 473-480.
23. E. K. Goharshadi and M. Hadadian, *Ceram. Int.*, 2012, **38**, 1771-1777.
24. E. K. Goharshadi, T. Mahvelati and M. Yazdanbakhsh, *J. Iran. Chem. Soc.*, 2015, 1-8.
25. P. Scherrer, *Nachr. Ges. Wiss. Göttingen*, 1918, **2**, 96-100.
26. C. H. Li and G. Peterson, *J. Appl. Phys.*, 2006, **99**, 084314.
27. J. Knox and I. Grant, *Chromatographia*, 1987, **24**, 135-143.
28. M. Zhang, Z. Che, J. Chen, H. Zhao, L. Yang, Z. Zhong and J. Lu, *J. Cem. Eng. Data.*, 2010, **56**, 859-864.
29. G. Huang, Y. Zhang, J. Ouyang, W. R. Baeyens and J. R. Delanghe, *Anal. Chim. Acta.*, 2006, **557**, 137-145.
30. Y. Guo, L. Huang, W. R. Baeyens, J. R. Delanghe, D. He and J. Ouyang, *Nano. Lett.*, 2009, **9**, 1320-1324.
31. M. Khafizov, I. W. Park, A. Chernatynskiy, L. He, J. Lin, J. J. Moore, D. Swank, T. Lillo, S. R. Phillpot and A. El-Azab, *J. Am. Ceram. Soc.*, 2014, **97**, 562-569.
32. J. L. Rupp and L. J. Gauckler, *Solid State Ionics*, 2006, **177**, 2513-2518.
33. J. F. Bisson, D. Fournier, M. Poulain, O. Lavigne and R. Mévrel, *J. Am. Ceram. Soc.*, 2000, **83**, 1993-1998.

34. G. Cao, *J. Appl. Electrochem.*, 1994, **24**, 1222-1227.
35. J. Liqiang, Q. Yichun, W. Baiqi, L. Shudan, J. Baojiang, Y. Libin, F. Wei, F. Honggang and S. Jiazhong, *Sol. Energ. Mat. Sol. C.*, 2006, **90**, 1773-1787.
36. V. Lazarev, V. Krasov and I. Shaplygin, Electrical Conductivity of Oxide Systems and Film Structures, Nauka, Moscow, 1979.
37. E. Pop, D. Mann, Q. Wang, K. Goodson and H. Dai, *Nano. Lett.*, 2006, **6**, 96-100.
38. Q. Li, Y. Li, X. Zhang, S. B. Chikkannanavar, Y. Zhao, A. M. Dangelewicz, L. Zheng, S. K. Doorn, Q. Jia and D. E. Peterson, *Adv. Mater.*, 2007, **19**, 3358-3363.
39. E. Goharshadi, H. Ahmadzadeh, S. Samiee and M. Hadadian, *Phys. Chem. Res*, 2009, **1**, 1-33.
40. R. Kochetov, A. Korobko, T. Andritsch, P. Morshuis, S. Picken and J. Smit, *J. Phys. D. Appl. Phys.*, 2011, **44**, 395401.
41. M. Abareshi, E. K. Goharshadi, S. M. Zebarjad, H. K. Fadafan and A. Youssefi, *J. Magn. Magn. Mater.*, 2010, **322**, 3895-3901.
42. J. Giddings, Unified Separation Science, chapter 8, p. 166, New York: John Wiley and Sons, 1991.
43. Y. Ito, J. Cazes, Encyclopedia of Chromatography, Taylor & Francis, 2001.
44. J. C. Reijenga, in *Encyclopedia of Chromatography, Second Edition*, Taylor & Francis, 2005, pp. 121-121.
45. D. C. Schwartz and C. R. Cantor, *Cell*, 1984, **37**, 67-75.
46. K. D. Cole and C. M. Tellez, *Biotechnol. Prog.*, 2002, **18**, 82-87.
47. Y. Kim and E. S. Yeung, *J. Chromatogr. A*., 1997, **781**, 315-325.
48. F. Han, B. H. Huynh, Y. Ma and B. Lin, *Anal. Chem.*, 1999, **71**, 2385-2389.
49. H. Zhou, A. W. Miller, Z. Sosic, B. Buchholz, A. E. Barron, L. Kotler and B. L. Karger, *Anal. Chem.*, 2000, **72**, 1045-1052.
50. A. E. Barron, D. S. Soane and H. W. Blanch, *J. Chromatogr. A*., 1993, **652**, 3-16.
51. B. Braun, H. W. Blanch and J. M. Prausnitz, *Electrophoresis*, 1997, **18**, 1994-1997.
52. W. Volkmuth and R. Austin, *Nature*, 1992, **358**, 600-602.
53. Y. Kim and M. D. Morris, *Anal. Chem.*, 1995, **67**, 784-786.
54. H. Oana, M. Ueda and K. Yoshikawa, *Electrophoresis*, 1997, **18**, 1912-1915.
55. J. Han and H. Craighead, *Science*, 2000, **288**, 1026-1029.
56. J. Han and H. G. Craighead, *Anal. Chem.*, 2002, **74**, 394-401.
57. C.-F. Chou, O. Bakajin, S. W. Turner, T. A. Duke, S. S. Chan, E. C. Cox, H. G. Craighead and R. H. Austin, *P. Natl. Acad. Sci.*, 1999, **96**, 13762-13765.
58. L. R. Huang, J. O. Tegenfeldt, J. J. Kraeft, J. C. Sturm, R. H. Austin and E. C. Cox, *Nat. Biotechnol.*, 2002, **20**, 1048-1051.
59. M.-F. Huang, Y.-C. Kuo, C.-C. Huang and H.-T. Chang, *Anal. Chem.*, 2004, **76**, 192-196.
60. H. Deng, X. Zhang, A. Kumar, G. Zou, X. Zhang and X.-J. Liang, *Chem. Commun.*, 2012, **49**, 51-53.
61. H. Li and L. Rothberg, *P. Natl. Acad. Sci. USA.*, 2004, **101**, 14036-14039.
62. W. Zhao, Y. Gao, M. A. Brook and Y. Li, *Chem. Commun.*, 2006, 3582-3584.
63. F. Zhao, H. Cheng, Y. Hu, L. Song, Z. Zhang, L. Jiang and L. Qu, *Sci. rep.*, 2014, **4**.
64. K. De Sitter, C. Dotremont, I. Genné and L. Stoops, *J. Membrane. Sci.*, 2014, **471**, 168-178.
65. K. Goren, L. Chen, L. S. Schadler and R. Ozisik, *J. Supercrit. Fluid*., 2010, **51**, 420-427.